

A massive reservoir of low-excitation molecular gas at high redshift

Padeli Papadopoulos,^{*} Rob Ivison,[†] Chris Carilli[‡] and Geraint Lewis^{||}

^{*} Leiden Observatory, PO Box 9513, 2300 Leiden, The Netherlands

[†] Department of Physics and Astronomy, University College London, Gower Street, London WC1E 6BT, UK

[‡] National Radio Astronomy Observatories, PO Box 0, Socorro, NM 87801-0387, USA

^{||} Anglo-Australian Observatory, PO Box 296, Epping, NSW 1710, New South Wales, Australia

Molecular hydrogen (H_2) is an important component of galaxies because it fuels star formation and accretion onto active galactic nuclei (AGN), the two processes that generate the large infrared luminosities of gas-rich galaxies^{1,2}. Observations of spectral-line emission from the tracer molecule carbon monoxide (CO) are used to probe the properties of this gas. But the lines that have been studied in the local Universe — mostly the lower rotational transitions of $J = 1 \rightarrow 0$ and $J = 2 \rightarrow 1$ — have hitherto been unobservable in high-redshift galaxies. Instead, higher transitions have been used, although the densities and temperatures required to excite these higher transitions may not be reached by much of the gas. As a result, past observations may have underestimated the total amount of molecular gas by a substantial amount. Here we report the discovery of large amounts of low-excitation molecular gas around

the infrared-luminous quasar, APM08279+5255 at $z = 3.91$, using the two lowest excitation lines of ^{12}CO ($J = 1 \rightarrow 0$ and $J = 2 \rightarrow 1$). The maps confirm the presence of hot and dense gas near the nucleus³, and reveal an extended reservoir of molecular gas with low excitation that is 10 to 100 times more massive than the gas traced by higher-excitation observations. This raises the possibility that significant amounts of low-excitation molecular gas may lurk in the environments of high-redshift ($z > 3$) galaxies.

APM08279+5255 was discovered serendipitously during a search for Galactic halo carbon stars⁴. It comprises a strongly lensed broad absorption line quasar at $z = 3.9$ with a complex optical spectrum and a bolometric luminosity of $\sim 10^{14} L_{\odot}$ (where L_{\odot} is the luminosity of the Sun) after correcting for lensing magnification; it displays extremely strong rest-frame far-infrared emission⁵ suggestive of dust-rich gas undergoing rapid star formation. The CO(4 \rightarrow 3) and CO(9 \rightarrow 8) lines have been detected³ suggesting that the molecular gas must be warm, extended on a scale of up to $1''$ in the image plane (only 160–270 pc in the source plane), with a mass of $(1 - 6) \times 10^9 M_{\odot}$.

We have used the National Radio Astronomy Observatory’s Very Large Array (VLA) to detect and image CO $J=1\rightarrow 0$ and $J=2\rightarrow 1$ emission from APM08279+5255. Emission in the CO(1 \rightarrow 0) line (Fig. 1) extends over scales of $\sim 7''$ (~ 30 kpc at $z = 3.9$ for $H_0 = 75 \text{ km s}^{-1} \text{ Mpc}^{-1}$, $q_0 = 0.5$), well beyond the gravitationally lensed nucleus⁶ where the emission from the CO(4 \rightarrow 3) and CO(9 \rightarrow 8) transitions is confined³. Maps of CO(2 \rightarrow 1) detect the northern part of the extended emission and show it to consist of two kinematically and spatially distinct features (Fig. 2). The continuum emission detected at

23 GHz emanates from the lensed nucleus and is unresolved ($\leq 0.6''$) with a flux density of 0.30 ± 0.05 mJy. At 43 GHz, no continuum emission is detected at a level of $\sigma = 0.30$ mJy, and the emission expected from the hot dust in the nucleus⁵ is negligible (≤ 0.04 mJy). No appreciable dust continuum is expected underlying the extra-nuclear CO(2→1) emission from the cooler dust/gas in those regions.

The nuclear CO(1→0) line emission has a velocity-integrated flux density of 0.150 ± 0.045 Jy km s⁻¹ and a deconvolved size of $\sim 0.6'' - 1''$, confirmed by the CO(2→1) map (Fig. 2) which shows this emission extending $\sim 0.8''$ along the direction expected from matched-resolution 1.6- μ m Hubble Space Telescope (HST) images⁶. This size is similar to that of the CO(4→3) and CO(9→8) emission³, while the velocity-averaged brightness temperature ratios, $R_{4\rightarrow3} = (4 \rightarrow 3)/(1 \rightarrow 0)$ and $R_{2\rightarrow1} = (2 \rightarrow 1)/(1 \rightarrow 0)$, are 1.5 ± 0.5 and 1.35 ± 0.55 , respectively, values perfectly compatible with a hot and dense gas phase in the nucleus.

We have considered in detail, and rejected, gravitational lensing as the cause of the extended CO(2→1) structure. There are no obvious optical counterparts and the CO(2→1) maps demonstrate that the two features to the north and north-east and the quasar nucleus do not share a common CO(2→1) line profile, a necessary characteristic if a single galaxy underlies them all. Detailed modeling of the lens^{6,7}, based on high-resolution HST and Keck data, does not suggest the existence of additional lensed features. We thus conclude that the extra-nuclear features are due to companion galaxies near APM 08279+5255. Moreover, their large angular distance from any central lens caustics precludes significant magnification (employing an elliptical mass distribution to represent the lensing galaxy⁶,

which accurately recovers the quasar image configuration, the magnification in this region is ≤ 1.2) and hence the implied molecular gas masses are large.

X_{CO} is the so-called CO-to- H_2 conversion factor^{8,9,10}, ranging from $\sim 1 M_{\odot} (\text{K km s}^{-1} \text{ pc}^2)^{-1}$ in ultraluminous infrared galaxies¹¹ (ULIRGs) to $\sim 5 M_{\odot} (\text{K km s}^{-1} \text{ pc}^2)^{-1}$ for quiescent spirals. The integrated flux density of the two extra-nuclear features in the CO(2 \rightarrow 1) maps is $1.15 \pm 0.54 \text{ Jy km s}^{-1}$ which (for the aforementioned range of X_{CO} and $R_{2\rightarrow 1} \sim 1$) yields a mass of $M(\text{H}_2) \sim (0.65 - 3.2) \times 10^{11} M_{\odot}$, this value being merely a lower limit if sub-thermal excitation of CO(2 \rightarrow 1) ($R_{2\rightarrow 1} < 1$) or sub-solar metallicities ($X_{\text{CO}} > 5 M_{\odot} (\text{K km s}^{-1} \text{ pc}^2)^{-1}$) are important.

This molecular gas reservoir is ~ 10 – 100 times more massive than that deduced for the nuclear region³ and neither CO(4 \rightarrow 3), CO(9 \rightarrow 8) nor high-resolution 210-GHz continuum maps give any hint of it. This mass is comparable to that of an entire spiral galaxy and is confined within $2'' - 3''$ or $\sim 10 \text{ kpc}$ (Fig. 2). Similar gas-rich companions with no obvious optical counterparts, akin to the recently discovered submillimetre galaxy population¹², have been found in the vicinity of other high-redshift systems^{13,14}. They have the tell-tale marks of intense ($L_{\text{FIR}} \sim 10^{13} L_{\odot}$), heavily obscured starbursts in merger configurations, converting a large reservoir of molecular gas ($\sim 10^{11} M_{\odot}$) into stars. In these systems the dynamical mass is comparable to the gas mass, a situation possible for the companion galaxies to APM 08279+5255, though only observations with higher spatial resolution and wider velocity coverage can address this issue properly.

The failure of sensitive spectral-line observations to detect any extra-nuclear CO(4 \rightarrow 3) and CO(9 \rightarrow 8) emission implies low values (≤ 0.15) for the global $R_{4\rightarrow 3}$ and $R_{9\rightarrow 8}$ ratios

for the massive reservoirs of molecular gas near APM 08279+5255. This has far-reaching consequences: at $z > 3$, millimetre-wave telescopes can only access CO $J + 1 \rightarrow J$, $J > 2$ and hence cannot hope to trace the bulk of the H₂ gas.

The low excitation of lines such as CO(9→8) is hardly surprising, even for a starburst environment, since the *average* conditions in the molecular gas will not be sufficient for their large-scale excitation. If the physical conditions in Orion A¹⁵ are typical of a starburst environment, $R_{9 \rightarrow 8} \leq 0.15$ (and in most cases $R_{9 \rightarrow 8} \leq 0.05$). Moreover, the molecular interstellar medium in intense starburst environments may not be just an ensemble of warm and dense Orion-type clouds. Where the most energetic star formation takes place, the gas may also have a warm but diffuse phase^{11,16}, $n(\text{H}_2) \leq 10^3 \text{ cm}^{-3}$, generated by the disruptive effects of intense ultraviolet radiation, supernovae and the violent dynamics associated with mergers. The CO $J + 1 \rightarrow J$, $J > 2$ emission from such gas will be weak, possibly for the entire starburst if this phase is dominant. Starbursts with similar far-infrared and low- J CO luminosities can be dominated by drastically different gas phases^{17,18}. Such differences are expected to occur during the evolution of a starburst, depending on the complex interplay between the accumulation of dense gas that feeds the star formation (for example, through a merger) and the cloud disruption caused by the products of that process, the massive stars.

Finally, since CO observations at high redshift usually sample emission averaged over several kiloparsecs, the possibility of cold and/or diffuse gas dominating the *global* CO emission should not be discounted. The CO $J + 1 \rightarrow J$, $J > 2$ transitions may then have low excitation and thus be very faint, a state not altered by the enhanced cosmic microwave

background¹⁴. The detection of CO at $z > 3$ means that significant metal-enrichment has taken place; low-excitation gas would then represent a previously metal-enriched part of its interstellar medium that is not participating in the observed star-formation episode. Such excitation gradients have been found in several nearby infrared-luminous galaxies hosting powerful circum-nuclear starbursts and AGN¹⁹.

APM08279+5255 can be seen as an extreme case of such an excitation gradient, further exaggerated by gravitational lensing of a particularly hot region of the underlying system. Differential lensing seems to be preferentially boosting the far-infrared and CO emission of the AGN-heated (rather than the starburst-heated) component of the interstellar medium. This is strongly suggested by the high temperature of the gas and dust (~ 200 K) which is not typical of nearby starbursts²⁰ or clouds heated by young stars (e.g. Orion A, $T \sim 40 - 60$ K). Also, the ratio $L_{\text{FIR}}/M(\text{H}_2) \sim 10^4 L_{\odot} M_{\odot}^{-1}$ is ~ 40 times higher than the highest values observed in ULIRGs and the $L_{\text{FIR}}/L_{1.4\text{GHz}}$ ratio is an order of magnitude larger than in star-forming galaxies. This all suggests a heating source other than stars and the AGN is the obvious alternative. Differential magnification of AGN-heated gas therefore seems to be responsible for the high luminosity of the CO(9 \rightarrow 8) line.

While highly excited regions with CO emission amplified by gravitational lensing are good markers of the presence of molecular gas at high redshifts, they may give a poor representation of its average physical conditions, particularly of its total mass and distribution. At $z > 3$, this excitation bias becomes more serious since millimetre-wave interferometers, the instruments usually used for such searches, can detect only CO $J+1 \rightarrow$

$J, J > 2$ whose excitation requirements are $n(\text{H}_2) \geq 10^4 \text{ cm}^{-3}$ and $T \geq 50 \text{ K}$. These values, being typical of the average conditions in star-forming clouds, mark a gradual excitation turnover.

Observations of the CO(1→0) and CO(2→1) transitions, with their minimal excitation requirements, may reveal much larger molecular gas reservoirs at high redshifts. The VLA is currently the only instrument capable of sensitive, sub-arcsecond observations of these lines and will thus be an important tool for unbiased surveys of metal-enriched H₂ gas around objects in the distant Universe²¹.

Methods.

Our observations took place during 23–24 April 2000 using the VLA in its C configuration. After all overheads, 20 hours were spent integrating on APM08279+5255. 19 of the 27 antennas were equipped with 43-GHz receivers ($T_{\text{sys}} = 45\text{--}100 \text{ K}$); all were equipped with 22-GHz receivers, including eleven new receivers with $T_{\text{sys}} \sim 40 \text{ K}$ (c.f. 100–150 K for the remainder).

We exploited the new fast-switching technique^{22,23}, recording data every 3.3 s, with 30 s on the calibrator and 170 s on the source (210 s in the 22-GHz band); the typical slewing overhead to the compact phase calibrator, 0824+558, 3.3° away, was 7 s. Pointing accuracy was checked every hour.

This technique yields diffraction-limited images at the highest VLA operating frequencies over long baselines. Conventional phase referencing would not have been able to

track tropospheric phase variations and self-calibration techniques could not be employed because of the low signal-to-noise per baseline.

We used continuum mode, placing emphasis on sensitivity rather than line profile information. A dual-polarisation 50-MHz band was placed as close to the expected line centre as could be allowed by correlator limitations: 23.4649 GHz for CO $J=1\rightarrow 0$ (+91 km s⁻¹ from the line centre³). Bandpass roll-off limited the effective bandwidth per IF to ~ 45 MHz which, at $z = 3.9$, corresponds to $\Delta v \sim 575$ km s⁻¹ at 23 GHz. The remaining IF pair was tuned to *simultaneously* observe the continuum at 23.3649 GHz (+1280 km s⁻¹).

We obtained matching velocity coverage at 43 GHz (CO $J=2\rightarrow 1$) by placing two contiguous 50-MHz dual-polarisation bands at 46.9399 GHz (-20 km s⁻¹ from the line centre). The continuum was observed on a separate occasion with both IF pairs tuned to 43.3 GHz. The flux density scale was fixed using 3C286; the uncertainty is $\sim 15\%$ at 23 GHz and $\sim 20\%$ at 46 GHz. Calibration and reduction of the data was standard in most respects and the rms noise in all the maps is similar to the expected theoretical limit.

We cannot completely rule out the possibility that phase errors — caused by atmospheric fluctuations too fast to be tracked even by our fast-switching scheme — are the cause of the extended CO emission, but we consider it remote. This is borne out by an extensive series of tests: inspection of the raw visibilities; separate imaging of left- and right-hand polarization maps; imaging of the most phase-stable subset of the data; imaging of the calibrator source. The agreement between the nuclear CO $J = 2 - 1$ emission and its associated 3.5-cm continuum is also strong testimony to the coherence of the CO $J = 2 - 1$ map; the point-like 23.4-GHz continuum emission, observed simultaneously with

the neighbouring line emission, provides similar supporting evidence for the resolved CO $J = 1 - 0$ emission.

References.

1. Telesco, C. M. Enhanced star formation and infrared emission in the centers of galaxies. *Ann. Rev. Astron. & Astrophys.* **26**, 343–376 (1988).
2. Sanders, D. B., Scoville, N. Z. & Soifer, B. T. Molecular gas in luminous infrared galaxies. *Astrophys. J.* **370**, 158–171 (1991).
3. Downes, D., Neri, R., Wiklind, T., Wilner, D. J. & Shaver, P. A. Detection of CO(4–3), CO(9–8), and dust emission in the broad absorption line quasar APM 08279+5255 at a redshift of 3.9. *Astrophys. J.* **513**, L1–L4 (1999).
4. Irwin, M. J., Ibata, R. A., Lewis, G. F. & Totten, E. J. APM 08279+5255: an ultraluminous broad absorption line quasar at a redshift $z = 3.87$. *Astrophys. J.* **505**, 529–535 (1998).
5. Lewis, G. F., Chapman, S. C., Ibata, R. A., Irwin, M. J. & Totten, E. J. Submillimeter observations of the ultraluminous broad absorption line quasar APM 08279+5255. *Astrophys. J.* **505**, L1–L5 (1998).
6. Ibata, R. A., Lewis, G. F., Irwin, M. J., Lehár, J. & Totten, E. J. NICMOS and VLA observations of the gravitationally lensed ultraluminous BAL quasar APM 08279+5255: detection of a third image. *Astron. J.* **118**, 1922–1930 (1999).
7. Egami, E. *et al.* APM 08279+5255: Keck near- and mid-infrared high-resolution imaging. *Astrophys. J.* **535**, 561–574 (2000).
8. Young, J. S. & Scoville, N. Z. Extragalactic CO — gas distributions which follow the light in IC 342 and NGC 6946. *Astrophys. J.* **258**, 467–489 (1982).

9. Young, J. S. & Scoville, N. Z. Molecular gas in galaxies. *Ann. Rev. Astron. & Astrophys.* **29**, 581–625 (1991).
10. Dickman, R. L., Snell, R. L. & Schloerb, F. P. Carbon monoxide as an extragalactic mass tracer. *Astrophys. J.* **309**, 326–330 (1986).
11. Downes, D. & Solomon, P. M. Rotating nuclear rings and extreme starbursts in ultraluminous galaxies. *Astrophys. J.* **507**, 615–654 (1998).
12. Smail, I., Ivison, R. J. & Blain, A. W. A deep sub-millimeter survey of lensing clusters: a new window on galaxy formation and evolution. *Astrophys. J.* **490**, L5–L8 (1997).
13. Ivison, R. J. *et al.* An excess of submillimeter sources near 4C 41.17: a candidate proto-cluster at $z=3.8$? *Astrophys. J.* **542**, 27–34 (2000).
14. Papadopoulos, P. P. *et al.* CO(4-3) and dust emission in two powerful high- z radio galaxies, and CO lines at high redshifts. *Astrophys. J.* **528**, 626–636 (2000).
15. Plume, R. *et al.* Large-scale $^{13}\text{CO } J=5-4$ and [C I] mapping of Orion A. *Astrophys. J.* **539**, L133–L136 (2000).
16. Aalto, S., Booth, R. S., Black, J. H. & Johansson, L. E. B. Molecular gas in starburst galaxies: line intensities and physical conditions. *Astron. & Astrophys.* **300**, 369–384 (1995).
17. Jackson, J. M., Paglione, T. A. D., Carlstrom, J. E. & Rieu, N. Submillimeter HCN and HCO+ emission from galaxies. *Astrophys. J.* **438**, 695–701 (1995).
18. Paglione, T. A. D., Jackson, J. M. & Ishizuki, S. The average properties of the dense molecular gas in galaxies. *Astrophys. J.* **484**, 656–663 (1997).

19. Papadopoulos, P. P. & Allen, M. L. Gas and dust in NGC 7469: submillimeter imaging and CO $J=3-2$. *Astrophys. J.* **537**, 631–637 (2000).
20. Hughes, D. H., Gear, W. K. & Robson, E. I. The submillimetre structure of the starburst nucleus in M82 — a diffraction-limited 450-micron map. *Mon. Not. R. Astron. Soc.* **270**, 641–649 (1994).
21. Ivison, R. J., Papadopoulos, P. P., Seaquist, E. R. & Eales, S. A. A search for molecular gas in a high-redshift radio galaxy. *Mon. Not. R. Astron. Soc.* **278**, 669–672 (1996).
22. Carilli, C. L. & Holdaway, M. A. Tropospheric phase calibration in millimeter interferometry. *Radio Science* **34**, 817–840 (1999).
23. Carilli, C. L., Menten, K. M. & Yun, M. S. Detection of CO(2–1) and radio continuum emission from the $z = 4.4$ QSO BRI 1335–0417. *Astrophys. J.* **521**, L25–L28 (1999).

Acknowledgments.

PP and RI would like to acknowledge many useful discussions and the early encouragement of Dr Ernie Seaquist. We are also indebted to Dr Richard Barvainis. The National Radio Astronomy Observatory is a facility of the National Science Foundation, operated under cooperative agreement by Associated Universities, Inc.

Correspondence and requests for materials should be addressed to Rob Ivison (rji@star.ucl.ac.uk).

Figure Captions.

Figure 1. Molecular gas in and around APM 08279+5255, as traced by CO $J=1\rightarrow 0$, and continuum emission from the active nucleus. *Top:* Naturally-weighted maps at $\nu_{\text{obs}} = 23.4649$ GHz, *middle:* $\nu_{\text{obs}} = 23.3649$ GHz, corresponding to CO $J=1\rightarrow 0$ ($\nu_{\text{rest}} = 115.2712$ GHz) and its adjacent continuum, respectively, at $z = 3.912$. The maps were produced from the Fourier transform of the measured visibilities, tapered to enhance low brightness extended emission. The dirty beam, identical in both maps with FWHM $1.5'' \times 1.4''$, is shown bottom left. Contours are at $-3, -2, 2, 3, 4, 5, 6, 8, 10 \times \sigma$, where $\sigma = 40 \mu\text{Jy beam}^{-1}$. *Bottom:* Naturally-weighted map of CO $J=1\rightarrow 0$ with the continuum source subtracted. The subtraction was performed in the visibility domain and the resulting uv data were then Fourier transformed, CLEANed and convolved to a circular beam, FWHM $2.25''$, shown bottom left. Contours this time are at $-3, -2, 2, 3, 4, 5, 6 \times \sigma$. The cross marks the position of lens⁶ component ‘A’ at RA 08h 31min 41.64s and Dec. $+52^\circ 45' 17.5''$ (J2000). The $0.5''$ offset between the peak radio intensity and ‘A’ is most likely due to *HST* astrometric errors.

Figure 2. Molecular gas in and around APM 08279+5255, as traced by CO $J = 2 - 1$, overlaid on a greyscale image of 8.45-GHz continuum emission from the active nucleus. *Top:* Naturally-weighted map of CO $J=2\rightarrow 1$ ($\nu_{\text{rest}} = 230.5380$ GHz) with both IF bands averaged (contours) and overlaid on continuum emission at 8.45 GHz (greyscale) at a common resolution ($0.5'' \times 0.5''$). Contours are at $-3, -2, 2, 3, 4, 5 \times \sigma$, where $\sigma = 0.15 \text{ mJy beam}^{-1}$ and the greyscale range is $25(2\sigma) - 305 \mu\text{Jy beam}^{-1}$. CLEAN was applied. *Bottom:* Naturally-weighted, tapered maps of CO $J=2\rightarrow 1$ for the two IF bands separately, at a common resolution of $0.90'' \times 0.75''$ FWHM. Contours are at $-3, 3, 4, 5, 6 \times \sigma$, where $\sigma = 0.20 \text{ mJy beam}^{-1}$. CLEAN was not applied. In all cases, the beam FWHM is shown bottom left and the cross marks the position of lens⁶ component ‘A’.

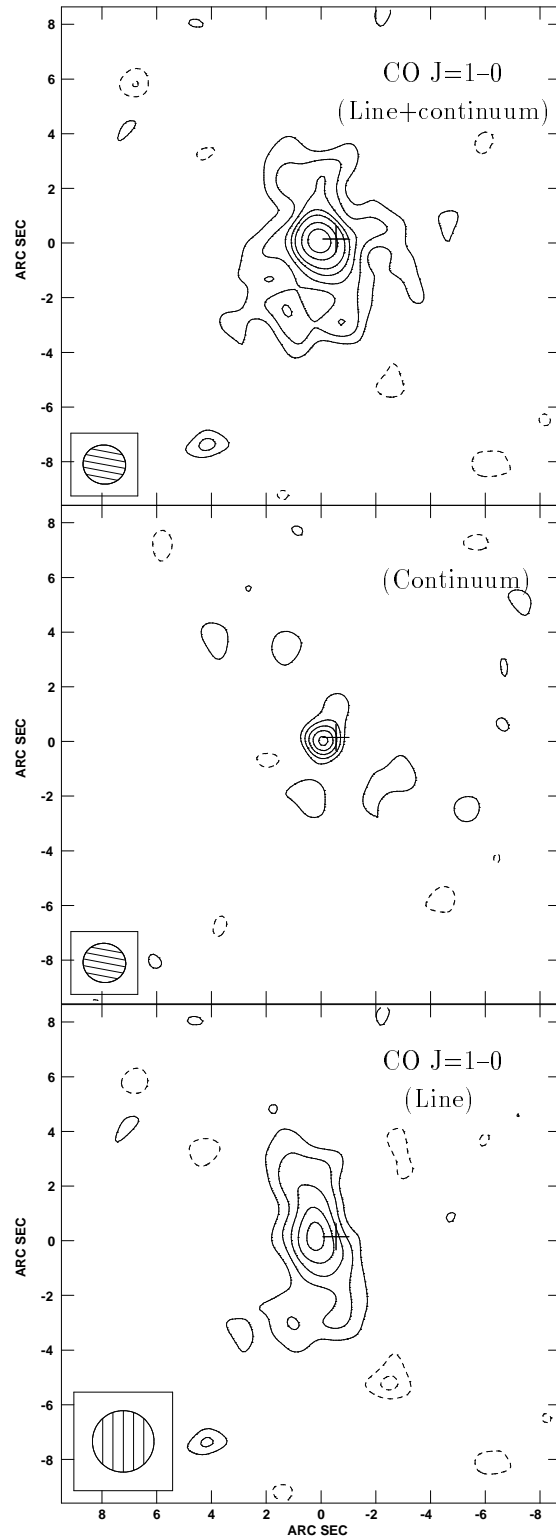


Figure 1

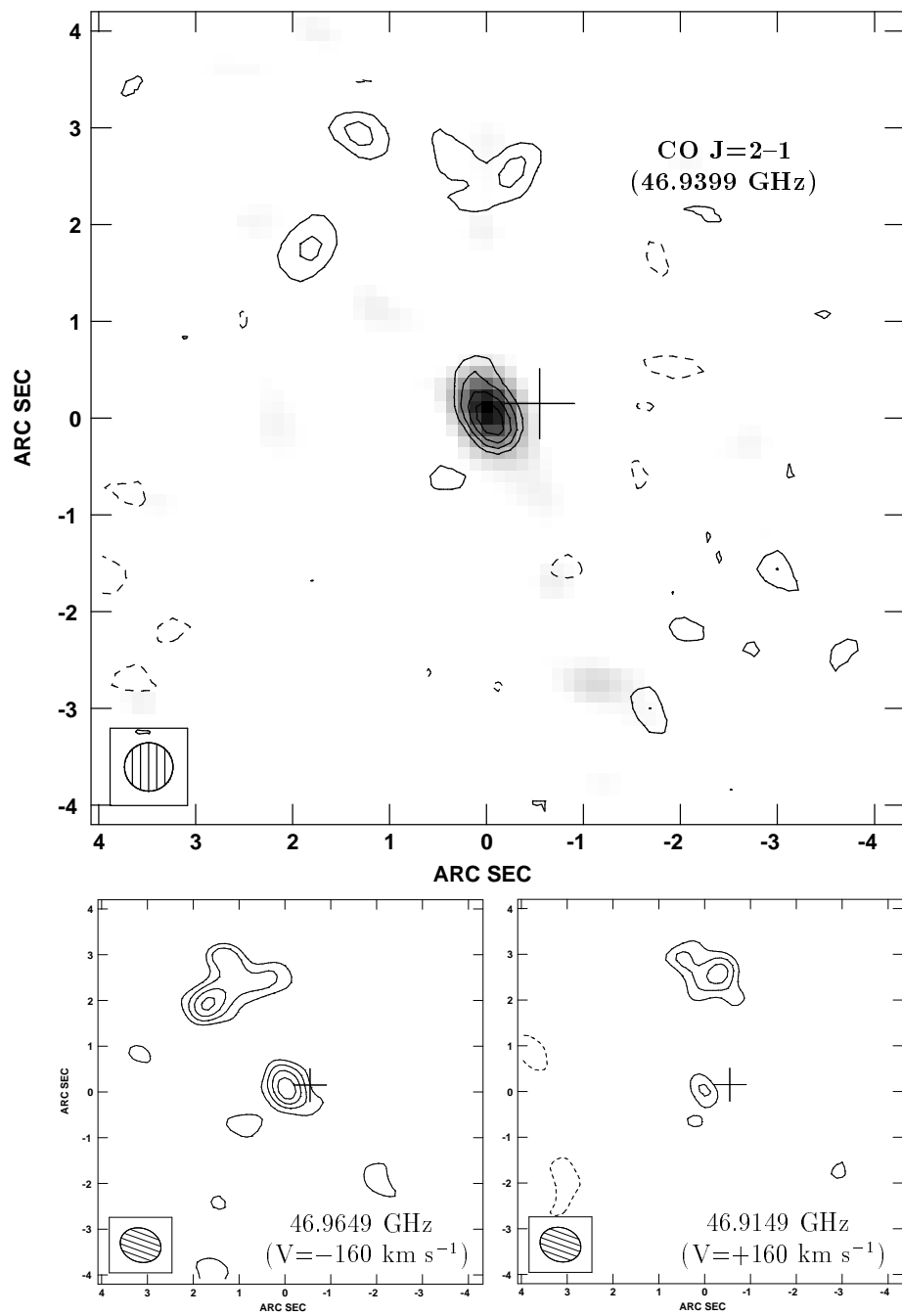


Figure 2